Project 4 - SI1336 Simulation and Modelling
Electrostatics and the Laplace equation

Raymond Wang

December 6, 2020

10.10 - Potential within a rectangular region

10.10a) Iterations for tolerance

The potential $V(x, y)$ in a square region with linear dimension 10 and boundary potentials $V = 10$ is to be determined. The grid size can be chosen as $n \times n$. In this case, one is to find the exact solution for the boundary problem:

$$\begin{cases} \nabla^2 V(x, y) = 0 \\ V(0, y) = V(11, y) = V(x, 0) = V(x, 11) = 10 \\ 0 \leq x, y \leq 11 \end{cases} \tag{1}$$

The exact solution is trivial and is given as

$$V_{exact}(x, y) = 10, \tag{2}$$

for the inner potentials. In order to solve numerically, an initial guess is set to a 10% lower inner potential, i.e:

$$V_{initial}(x, y) = 9. \tag{3}$$

Subsequently, the number of necessary iterations for 1 % accuracy is to be determined. The accuracy can be interpreted as the tolerance criterion and is calculated as:

$$\left| \frac{V(i, j) - V_{exact}(i, j)}{V_{exact}(i, j)} \right| < 0.01, \tag{4}$$

with $1 \leq i$ and $j \leq n$. The numerical solver utilizes a relaxation method with finite difference discretizations. Iterations can as such be interpreted as relaxations and with this framework, the potential field is iterated for grid sizes $n \in [2, 30]$, $n \in \mathbb{N}$. The results are illustrated using Cartesian as well as log-log plots.

Relaxations for tolerance

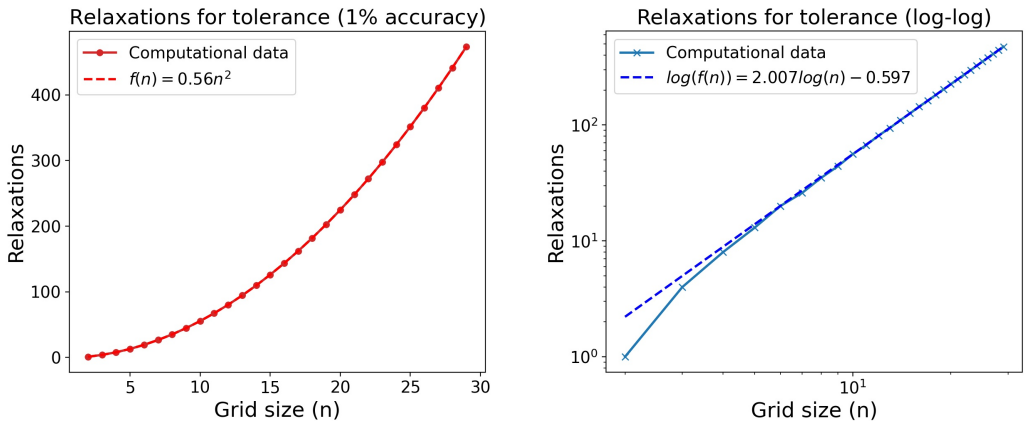

(a) (b)

Figure 1: (a) Quadratic plot (b) Log-log-plot

Regressions have been fitted for the computational data, showing that 13 relaxations are required for grid size $n = 5$ and 56 relaxations for $n = 10$. For large grid sizes, the relation converges toward $f(n) = 0.56n^2$. This correlation can also be derived from converting the linear log-log function into a monomial.

10.10b) Alternate inner potentials

Consider the same geometry as in part (a), but set the initial potential at the interior sites equal to 0 except for the center site whose potential is set equal to 4. In these conditions, a poor initial guess can be set as (3) while a good initial guess can be defined as:

$$V(n/2, n/2) = 4, \tag{5}$$

for even n and

$$\begin{cases} V(n/2, n/2) = 4 \\ V(n/2+1, n/2) = 4 \\ V(n/2, n/2+1) = 4 \\ V(n/2+1, n/2+1) = 4, \end{cases} \tag{6}$$

for odd n. As in the previous case, the required iterations for various grid-sizes will be plotted and compared.

Relaxations for tolerance

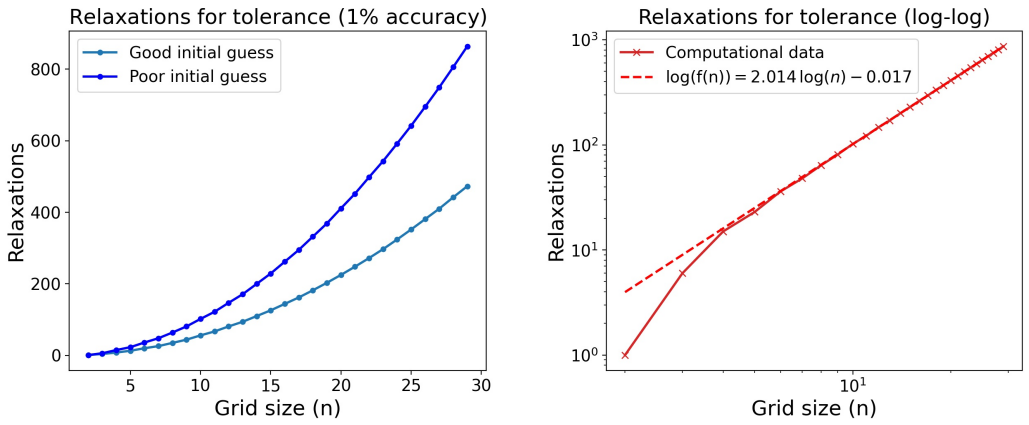

(a) (b)

Figure 2: (a) Quadratic plot (b) Log-log-plot

It should be noted that a poor initial guess require more relaxations to attain the tolerance criterion and from the log-log-plot, the correlation between grid size and relaxations can be derived as: $\sim n^2$. In order words, the required relaxations is proportional to the area of the grid for large n. As a matter of fact 23 iterations were required for $n = 5$ and 102 for $n = 10$.

Since every point in each relaxation step is computed as the average of its 4 surrounding neighbors, no change is only fulfilled when $V(x, y) = 10$. Thus, it can be argued that the final results are independent of the initial guesses.

10.10c) Equipotential surfaces

The equipotential surfaces for two boundary conditions are to be sketched. For the first one, the potential at the four sides is 5, 10, 5, and 10 respectively, while the potential is 10 on three sides and 0 on the fourth, for the second one. The initial guess for the first boundary condition is set to:

$$V_{initial}(x, y) = 7.5, \tag{7}$$

for inner potentials. As for the grid size, the same as previously ($n = 10$) is to be utilized for the equipotential surfaces.

For the second boundary condition, the initial guess is set to:

$$V(i,j) = 10 - \frac{10j}{n-1}, \tag{8}$$

in which $1 \leq i$ and $j \leq n$, for the inner potentials. In order to generate qualitative solutions without solving the initial value problem analytically, the tolerance criterion is defined as:

$$\left| \frac{V_n(i,j) - V_{n-1}(i,j)}{V_{n-1}(i,j)} \right| < 10^{-4}. \tag{9}$$

In this case a maximum deviation between subsequent iteration is 0.01%.

Equipotential surfaces

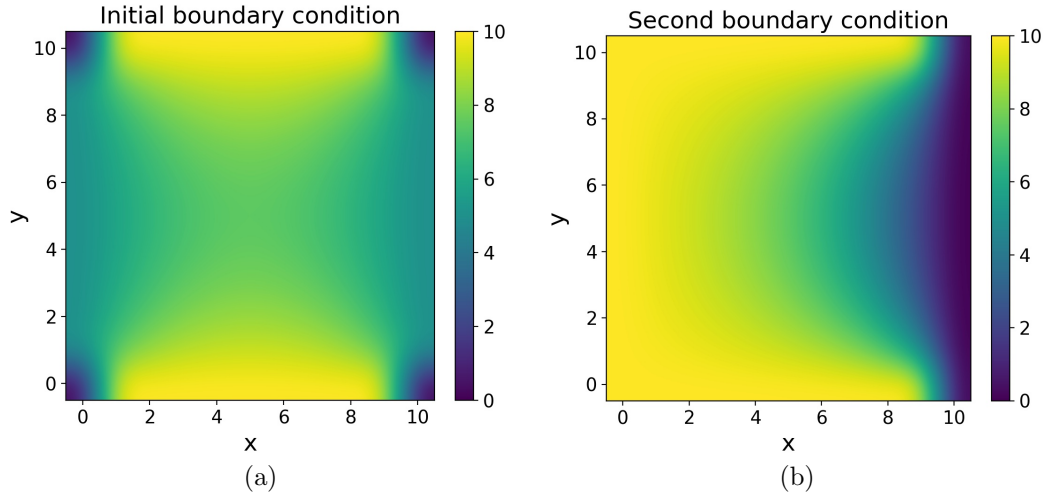

(a) (b)

Figure 3: (a) Initial boundary condition (b) Second boundary condition

As can be noted, the initial boundary condition shows greater potentials near the upper and lower boundaries of the surface while decreasing towards the middle. The corners have potentials 0. For the second boundary condition, the potential is greatest at the right corner while steadily decreasing as it traverses toward the left side.

Countour plots

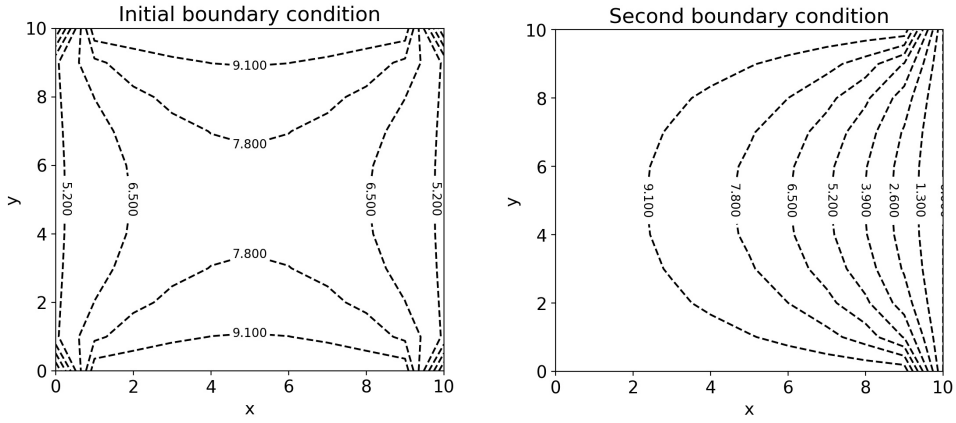

(a) (b)

Figure 4: (a) Initial boundary condition (b) Second boundary condition

10.11 - Gauss-Seidel relaxation

10.11a) Gauss-Seidel relaxation

Utilizing the same grid size, methods and tolerance criteria as in 10.10a, the previous relaxation method is to be compared with a Gauss-Seidel relaxation.

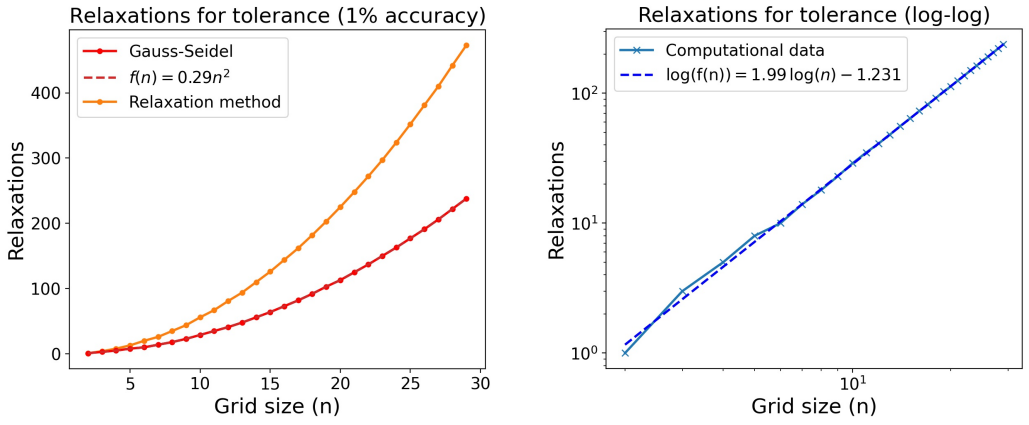

(a) (b)

Figure 5: (a) Initial boundary condition (b) Second boundary condition

A Gauss-Seidel relaxation is a modification upon the initial relaxation method. In this case, the potential at each site is sequentially updated and thus, the potential of the subsequent site can be computed by utilizing the most recently derived values for the potentials of its nearest neighbors.

As can be noted from the diagrams, this modification improves the Convergence. For $n = 5$, 8 relaxations were required and for $n = 10$, the necessary relaxations amounted to 20. Using relation, or alternatively the log-log-plot, the correlation between grid size and relaxations can be derived as $0.29n^2$. However, if one is to compare the respective equipotential surfaces, it can be noted that the Gauss-Seidel method yields slightly less accurate solutions as compare to the unmodified relaxation method.

10.11b) Checker relaxation

As for the Checker relaxation, alternate sites of the grid are colored red and black. The red site are initially updated and this ordering is repeated for each iteration.

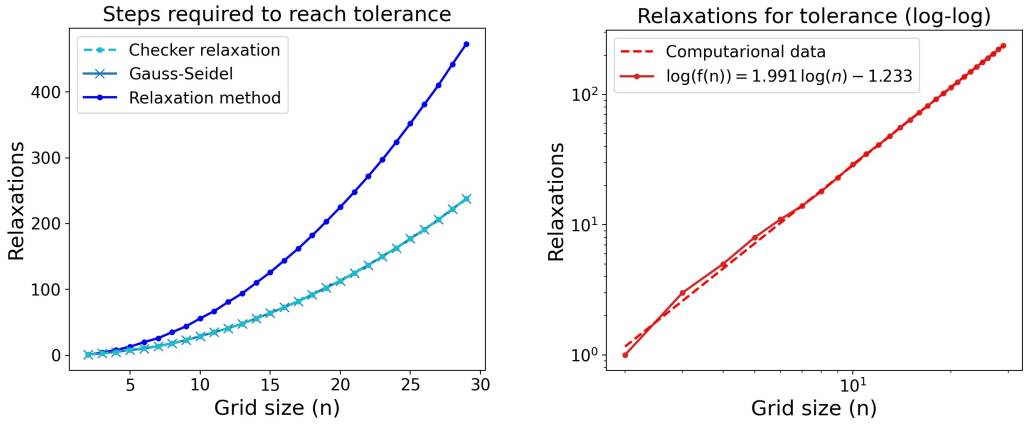

(a) (b)

Figure 6: (a) Quadratic plot (b) Log-log-plot

As can be noted, the convergence for the Checker relaxation correlates almost exactly with the Gauss-Seidel relaxation. For smaller grid sizes, it requires a few iterations less for convergence but this difference becomes negligible as n increases.

10.17 - Random-walk solution for Laplace's equation

The same grid and boundary conditions as in 10.10c is to be utilized. The random-walk-solutions are then compared with the highly accurate solution generated by the relaxation method

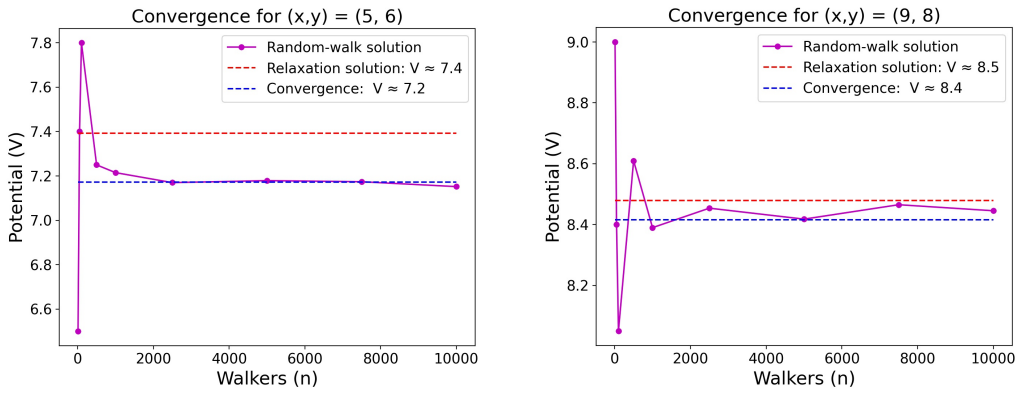

(a) (b)

Figure 7: (a) Convergence for $(x, y) = (5, 6)$ (b) Convergence for $(x, y) = (9, 8)$

As can be noted by choosing a point in the vicinity of the center, i.e. (5,4), the random-walk solutions converge to a lesser value as compared to the relaxation solution. The random walks converges for potential $V \approx 7.2$ while the more exact value generated by the relaxation method falls within $V \approx 7.4$.

For points farther from the center, i.e. (9.8), the expected value for the random- walk correlates more with the more exact value generated by the relaxation method. In this case, the deviation is only ~ 0.1 as compared to the 0.2 deviation from (5,4).

On that account, it can be concluded that the random-walk method generates more exact values for points farther away from the center of the grid while being less qualitative for points in a more central location. For both instance, at least 2000 walkers are required for the solutions to sufficiently converge. However, due to their random nature, each simulation of the random walks is different and this also applies for the convergence patterns. In this case, one can plot the standard error of the mean of the sampled potential values and compare the convergence behavior for the two given points.

Standard error of the mean

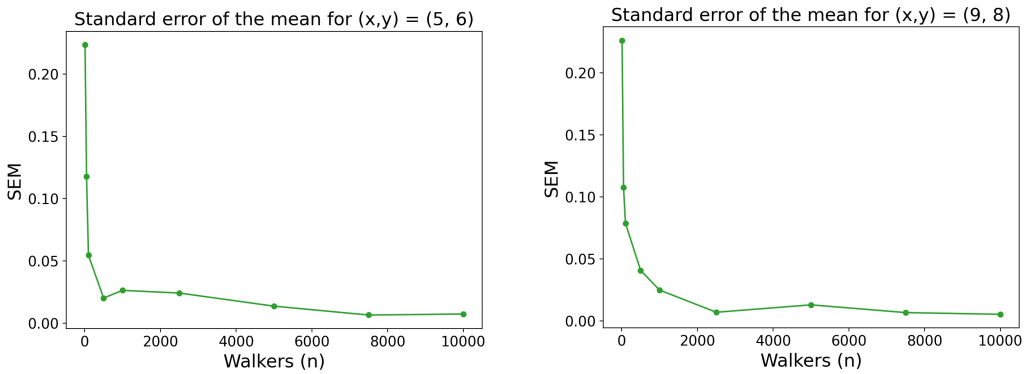

(a) (b)

Figure 8: (a) SEM for $(x, y) = (5, 6)$ (b) SEM for $(x, y) = (9, 8)$

As can be noted, the solutions for points farther away from the center (9,8) converges later and therefore, with less amount of walkers, n. For points in the vicinity of the center, the solutions converge sooner. As such, it can be concluded that the closer to the center a point it, the better it converges. Nonetheless. the convergence patterns for both instances are highly analogous and it can generally be considered that 1000 walkers are required for sufficiently converged solutions for the potentials.

10.18 - Green's function solution of Laplace's equation

10.18a) Estimation of Green's function

Utilizing the same geometry as in 10.10c, the Green function for various points is to be determined. In this case the quantity of interest is $G(x, y, x_b, y_b)$, the number of times that a walker from the point (x, y) lands at the boundary (x_b, y_b). In such case, $G(x, y, x_b, y_b)$ can be expressed as:

$$G(x, y, x_b, y_b) = \frac{nV(x, y)}{\Sigma_{x_b, y_b} V(x_b, y_b)}, \tag{10}$$

where n is the number of times that a walker from the point (x, y) lands at the boundary (x_b, y_b) and $V(x, y)$ the potential of the given point.

In order to numerically evaluate G, the random-walk algorithm has to be modified. In this case, the walkers return to the boundary site in case the values for x and y exceed the geometry of the region. Due to the symmetry of the geometry, some values for G can be derived from other values without additional calculations. En equipotential sketch of G yields:

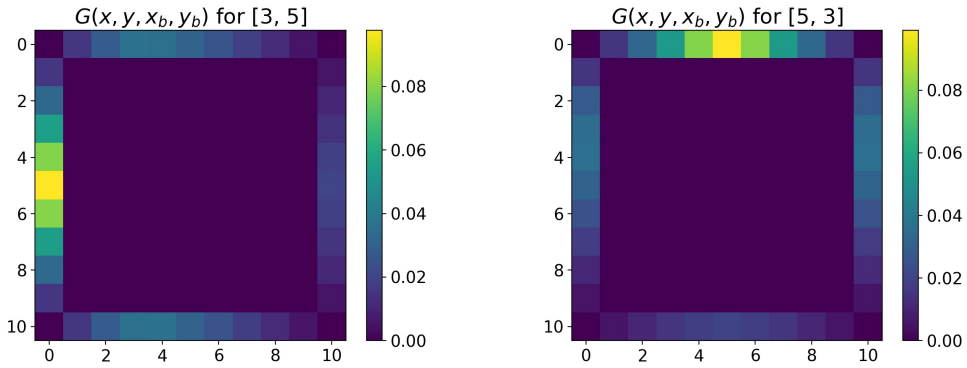

(a) (b)

Figure 9: (a) $(x, y) = (3, 5)$ (b) $(x, y) = (5, 3)$

As in the figures, every position indicates the fraction of random walks that ended up in that position.

10.18b) Maximizing potentials

The results for G can be utilizing in determining the potential of each interior site. In this instance, the potentials for five selected boundary sites for the geometry in 10.10c is set to $V = 20$ and the locations of the boundary sites that maximize the potential for (5,3) and (3,5) are to be determined. One can initially rewrite (10) to its ordinary form, i.e:

$$V(x, y) = \frac{1}{n} \sum_{x_b, y_b} G(x, y, x_b, y_b) V(x_b, y_b). \tag{11}$$

The estimations for G can subsequently be estimated using the same methodology as in 10.18a.

Boundary values maximizing potential

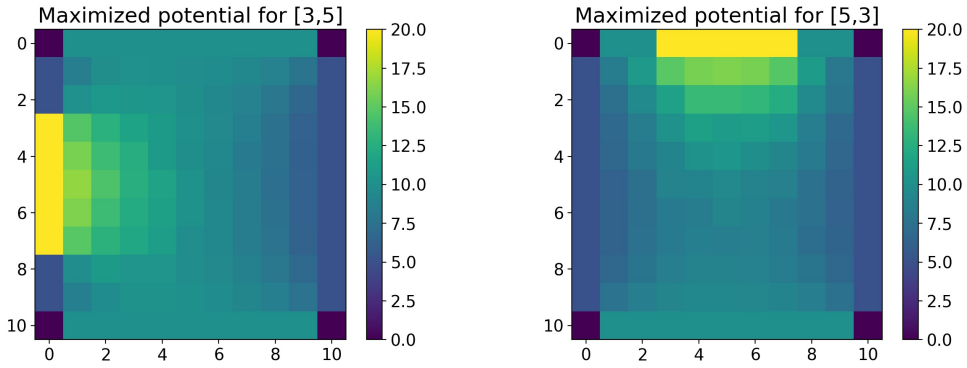

(a) (b)

Figure 10: (a) $(x, y) = (3, 5)$ (b) $(x, y) = (5, 3)$

Utilizing trial and error guided with physical intuition, it can be noted that the five boundary points maximizing the potential for $(3, 5)$ are: $(3, 0)$, $(4, 0)$, $(5, 0)$, $(6, 0)$ and $(7, 0)$. Likewise, the five boundary points maximizing the potential for $(5, 3)$ are $(0, 3)$, $(0, 4)$, $(0, 4)$, $(0, 5)$ and $(0, 7)$.